

Increased Oil Recovery from the Danish North Sea Chalk Fields Flooding Experiment OCD1 Final Report

Dan Olsen

2. revised edition



Increased Oil Recovery from the Danish North Sea Chalk Fields Flooding Experiment OCD1 Final Report

Dan Olsen

2. revised edition

Contents

1. SUMMARY	2
2. INTRODUCTION	3
3. EQUIPMENT	4
4. FLUIDS AND EXPERIMENTAL CONDITIONS	5
5. EXPERIMENT OCD1	7
5.1. EXPERIMENT SET-UP	7
5.2. INITIAL SAMPLE CHARACTERIZATION	8
5.3. FINAL SAMPLE CHARACTERIZATION	8
5.4. PERMEABILITY DETERMINATIONS	9
5.5. PRODUCTION OF OIL DURING THE FLOODINGS	10
5.6. WATERFLOODING	11
5.7. CO ₂ -ENRICHED FLOODING	12
5.8. COMPACTION AND DISSOLUTION STRUCTURES	18
6. REFERENCES	20

1. Summary

A complex flooding experiment was conducted on a chalk sample from the Nana-1XP well of the Danish North Sea. The chalk was low-permeability chalk from the Ekofisk Formation that is considered marginal to the Halfdan reservoir. The aim of the study was to test the efficiency of CO₂-enriched water to produce additional oil from such rocks.

The sample of the study consisted of four 1.5" plug samples that were assembled to a composite sample that is referred to as sample OCD1. The flooding experiment is referred to as experiment OCD1. It was conducted at a fluid pressure of 282 bara, a hydrostatic confining pressure of 429 bara, and a temperature of 85 °C. These are conditions similar to the conditions of the Halfdan oil reservoir. The experiment started with initial sample preparation followed by ageing at reservoir conditions. At the start of the flooding experiments the oil saturation of the sample, S_o , was 77.7 %PV (percent of pore volume). A waterflooding with 5.35 PV (pore volumes) of simulated formation water brought the S_o of the sample down to 28.1 %PV, i.e. 49.6 %PV of oil was produced. Waterflooding continued until the oil production had ceased. The experiment continued, now as a flooding with CO₂-enriched water, where the water was 100 % saturated with CO₂. During the CO₂-enriched flooding a total volume of 10.36 PV of CO₂-enriched water flowed through the sample. The measurement of the oil production during the flooding with CO₂-enriched water was troubled by disequilibrium within the separator of the reservoir condition rig, and a correction procedure was applied. Using the correction procedure, the CO₂-enriched flooding brought the S_o of the sample down to 23.3 %PV, i.e. 4.7 %PV of additional oil was produced. If the correction procedure is not used, the resulting S_o of the sample after the CO₂-enriched flooding is 24.8 %PV, i.e. 3.3 %PV of additional oil was produced. The results using the correction procedure are considered most reliable. No matter whether the correction procedure is used or not, the amount of additional oil produced by the CO₂-enriched flooding is small compared to the amount of oil produced by the waterflooding.

The present study shows that waterflooding works very efficiently even in this kind of low-permeability chalk. Compared to this, the use of CO₂-enriched water only produces small amounts of additional oil. It is emphasized that the results have no implications for the use of a supercritical CO₂-phase as a flooding agent.

At the inlet end of the rock sample a dissolution structure was created by the CO₂-enriched water. The rest of the sample appeared unaffected by the floodings, except for a minor increase in porosity and a 23 % increase in gas permeability. The sample length was reduced by 0.23 % during the two floodings.

2. Introduction

This report presents the results of the experimental work conducted at GEUS for the project "Increased Oil Recovery from the Danish North Sea Chalk Fields" that is financed by the Ministry of Science, Technology and Innovation. The project is coordinated by Offshore Center Danmark. The experimental work was conducted between 1. June 2006 and 1. June 2007.

The work of GEUS consisted of a complex flooding experiment that is for short referred to as experiment OCD1. The aim of the experiment was to test the efficiency of CO₂-enriched water in reducing the residual oil saturation of chalk with poor reservoir properties from the Halfdan field in the Danish North Sea.

Preparation of the samples for experiment OCD1 was started in June 2006. The reservoir condition part of the experiment was conducted from 4. December 2006 to 3. May 2007. Final sample characterization was conducted in May 2007.

The experimental plan was presented and discussed at a status meeting at Offshore Center Danmark on 24. October 2006. The experimental work in progress was presented and discussed at the Sub-soil Conference at Offshore Center Danmark on 6. February 2007 and at a status meetings at Offshore Center Danmark on 12. April 2007.

Sample material and experimental conditions were selected to avoid confidentiality restrictions. Therefore, the data of the present report may be cited without restrictions.

3. Equipment

The flooding experiments were conducted in a reservoir condition rig at GEUS that consisted of a Hassler-type core holder, a number of pressure cylinders for the experimental fluids, an acoustic separator for fluid production measurement, a differential pressure transducer for permeability measurement, and a high pressure pump system. The reservoir condition rig had the following specifications:

1. Maximum fluid pressure 690 bar.
2. Maximum temperature 121 °C.
3. Maximum hydrostatic confining pressure 690 bar.
4. Tolerance to saline CO₂ rich brine within pressure and temperature specifications.
5. Temperature stability better than 1 °C.
6. Flow accuracy better than 2 % of nominal rate.
7. Ability to measure differential pressure across the sample with accuracy better than 0.01 bar.
8. Ability to quantify fluid volumes in a 2-phase system with accuracy better than 0.1 ml.
9. Accepts 38 mm diameter core samples with lengths up to 45 cm.

Core holder, pressure cylinders, separator, and differential pressure transducer were all situated inside a large thermostated oven (Fig. 3.1). The oven provided very stable temperature control, i.e. significantly better than 1 °C, except when the oven doors were opened. When this happened the air temperature inside the oven dropped up to 40 °C, and caused thermal instability, that required up to 3 hours with closed doors to recover. For this reason the oven doors were kept closed during the critical parts of the experiments, in particular the core flooding operations.

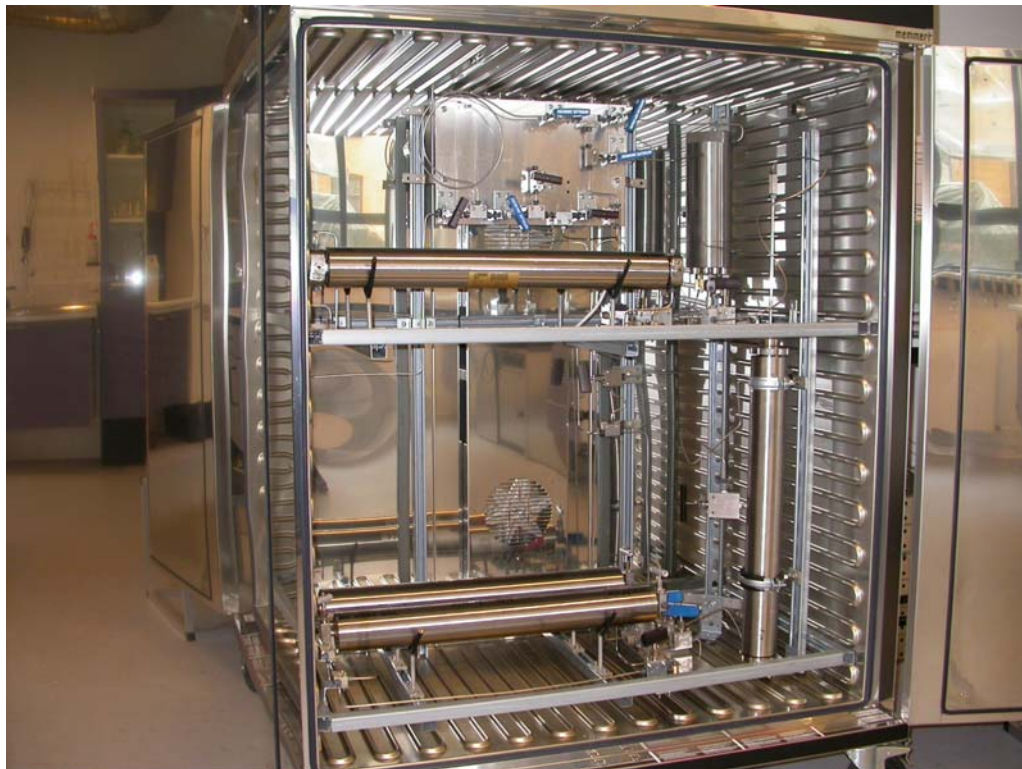


Fig. 3.1. GEUS reservoir condition rig.

4. Fluids and experimental conditions

The experimental conditions for experiment OCD1 are summarised in Table 4.1. The temperature and fluid pressure conditions were selected to be similar to the Dan Field reservoir (Jorgensen, 1991) with corrections for the slightly different depth of the Halfdan reservoir: The temperature was corrected using a temperature gradient of 0.04 °C/m, and the fluid pressure was corrected using a pressure gradient of 0.075 bar/m.

All experimental data are corrected for the thermal expansion of the pressure medium that took place when the pressure medium flowed from the high-pressure pump that was situated at 23 °C, into the oven, and conversely corrected for thermal contraction when the pressure medium flowed from the oven back to the pump. The flow-rate of the high-pressure pump was checked versus the reading of the separator at reservoir conditions and the two flow-rates were found to deviate less than 1% from each other.

The oil used in experiment OCD1 was degassed crude oil from the Dan Field. Table 4.2 gives some petrophysical properties of the oil as determined at GEUS. The use of a degassed crude oil, rather than live oil, was not an ideal condition, but was forced by the economy of the project.

Table 4.1. Conditions for experiment OCD1.

Experiment id.	OCD1
Sample type	Composite 1.5" plug
Temperature	85 °C
Fluid pressure	282 bara
Hydrostatic confining pressure	429 bara
Flooding rate, waterflooding	0.62 ml/h
Flooding rate, CO ₂ -enriched flooding	0.62 ml/h
CO ₂ contents of brine, CO ₂ -enriched flooding	26.6 Sm ³ /Sm ³

Table 4.2. Properties of the degassed crude oil used for experiment OCD1.

Experiment id.	OCD1
Density (g/ml) @ 1 atm and 23 °C	0.882
Viscosity (cP) @ 85 °C	3.75

Table 4.3 presents the composition of the simulated formation water used for experiment OCD1. The brine simulated the composition of the formation water of the Halfdan Field. The density given in Table 4.3 was measured at GEUS using a Paar DMA 35 densitometer. The viscosity at reservoir conditions was estimated from the viscosity of similar brines.

The CO₂ used for the experiments had a purity of 99.99 %.

Table 4.3. Composition of simulated formation water.

Experiment id.	OCD1
Na ⁺ (mg/l)	17900
Ca ²⁺ (mg/l)	1420
Mg ²⁺ (mg/l)	493
K ⁺ (mg/l)	136
Cl ⁻ (mg/l)	31678
CO ₃ ⁻ (mg/l)	0
HCO ₃ ⁻ (mg/l)	500
TDS (mg/l)	51627
Density (g/ml) measured at GEUS @ 25 °C & 1 atm	1.032
Viscosity (cP) estimated @ 85 °C & 282 bara	0.460

5. Experiment OCD1

5.1. Experiment set-up

The experiment procedure for experiment OCD 1 is presented in Table 5.1.

During the experiment the following parameters were continuously logged:

- Differential pressure
- Pore fluid pressure
- Hydrostatic confining pressure
- Flow rate
- Cumulative fluid volume
- Position of water-oil interface in the separator
- Temperature

Table 5.1. Experimental procedure for experiment OCD1.

1. Selection of four 1.5" core plugs from the Nana-1XP well.
2. Cleaning of individual plugs.
3. Conventional core analysis of individual plugs.
4. Establish S_{wi} on individual plugs by the porous plate method using Isopar-L laboratory oil.
5. Photography of individual plugs.
6. Measure $k_o(S_{wi})$ on individual plugs with Isopar-L.
7. Mount a composite core composed of the samples with identification nos. 21, 22, 23, and 29 in a core holder. The plugs are mounted with increasing permeability towards the outlet end of the core holder:
(inlet) 29 → 23 → 22 → 21 (outlet).
A good fit between the individual samples is aimed to assure good capillary contact.
8. Establish reservoir conditions: $P_{conf}=429$ bara, $P_{fluid}=282$ bara, $T=85$ °C.
9. Replace the Isopar-L oil of the core with Dan Crude oil by flushing with 3 pore volumes of crude oil.
10. Ageing for three weeks at reservoir conditions.
11. Measure permeability $k_o(S_{wi})$ at reservoir conditions.
12. Waterflooding. Flood the core with simulated formation water without CO₂ at a rate of 0.62 ml/h. Continue flooding until a stable $k_w(S_{or})$ is obtained. Logging of produced oil, V_o , temperature, T , flow-rate, Q_w , confining pressure, P_{conf} , fluid pressure, P_{fluid} , and differential pressure, ΔP .
13. CO₂-enriched flooding. Flood the core with 10 pore volumes of simulated formation water saturated with CO₂ at a rate of 0.62 ml/h. Logging as for the waterflooding.
14. Depressurize and cool down the rig. Dismount the core.
15. Photography of the core.
16. Dean Stark analysis of the individual core plugs to determine the final fluid saturation.
17. Conventional core analysis.

Table 5.2 OCD1, initial sample characterization.

Arrow indicates flow direction from bottom towards top of core.

Sample id.	Depth (m)	Dry wght (g)	Diameter (mm)	Length (mm)	Bulk vol. (ml)	Por (%BV)	Pore vol (ml)	Gr.dns. (g/ml)	kg (mD)	Swi (%PV)	Water cont. (ml)
Outlet end											
↑ 21	2117.6	150.49	37.64	71.29	80.24	30.57	24.53	2.701	0.82	19.5	4.8
22	2117.7	151.48	37.65	70.47	79.27	29.38	23.29	2.706	0.70	20.3	4.7
23	2117.7	154.78	37.64	70.66	79.46	27.97	22.22	2.704	0.57	24.8	5.5
29	2119.5	156.62	37.66	70.75	79.59	27.14	21.60	2.701	0.49	25.0	5.4
Inlet end											
Arithmetic mean value			37.65		28.77		2.703		0.65		22.4
Harmonic mean value									0.62		
Volume weighted mean						28.77		2.703		22.3	
Cumulative value		613.37		283.17		318.56		91.64		20.4	

Table 5.3. OCD1, final sample characterization.

Arrow indicates flow direction from bottom towards top of core.

Sample id.	Depth (m)	Dry wght (g)	Diam. (mm)	Length (mm)	Bulk vol. (ml)	Porosity (%BV)	Pore vol (ml)	Gr.dns. (g/ml)	kg (mD)	Sw (%PV)	So (%PV)	Sg (%PV)		
Outlet end														
↑ 21	2117.6	150.05	37.67	71.26	80.05	30.86	24.70	2.710	1.01	47.2	27.5	25.3		
22	2117.7	151.02	37.69	70.47	79.11	29.53	23.36	2.709	0.84	46.0	25.4	28.6		
23	2117.7	154.28	37.68	70.60	79.31	28.24	22.39	2.710	0.70	45.3	25.4	29.3		
29	2119.5	153.70	37.66	70.10	78.46	27.69	21.72	2.708	0.62	51.4	24.6	24.1		
Inlet end														
Arithmetic mean value			37.68		29.08		2.709		0.79		47.5	25.7	26.8	
Harmonic mean value									0.76					
Volume weighted mean						29.09		2.710		47.4		25.8		26.8
Cumulative value		609.05		282.43		316.92		92.18						

5.2. Initial sample characterization

Experiment OCD1 was conducted with a composite sample, sample OCD1, that consisted of four 1.5" plug samples from the Nana-1XP well of the Halfdan field in the Danish North Sea. Before the flooding experiment the basic data given in Table 5.2 were determined. The four sub-samples were mounted in the core holder in the sequence indicated by the first column of Table 5.2. The ordering was determined as the order of increasing gas permeability from the inlet end towards the outlet end. The core was mounted in a vertical position, and both the waterflooding and CO₂-enriched flooding took place from the bottom towards the top.

5.3. Final sample characterization

The sub-samples of composite sample OCD1 were characterized after the flooding experiment by the same conventional core analysis methods that were used for the initial characterization. Final sample characterization data are given in Table 5.3.

Table 5.4 summarizes the changes in some of the conventional core analysis parameters that took place during the flooding experiment. At the final characterization the composite sample had lost 4.3 g of weight relative to the initial characterization. The loss was caused by dissolution of material during the flooding experiments. Part of the loss occurred when

Table 5.4. OCD1 experiment, changes between initial and final characterization.

	Initial characterization	Final characterization	Change	Percent change
Dry weight (g)	613.37	609.05	-4.32	-0.70
Diameter (cm)	3.765	3.768	0.003	0.07
Length (cm)	28.317	28.243	-0.074	-0.26
Bulk volume (ml)	318.56	316.92	-1.64	-0.52
Porosity (%BV)	28.77	29.09	0.32	1.10
Pore volume (ml)	91.64	92.18	0.53	0.58
Gas perm (mD)	0.62	0.76	0.14	22.88

particles that had been detached by the dissolution process were lost during sample dismount. The total loss is equivalent to 0.70 % of the initial sample weight. A reduction in bulk volume is more than balanced by an increase in porosity, so that the pore volume of the sample actually increased slightly during the experiment. The length reduction occurred mainly in sub-sample 29 adjacent to the inlet end, cf. Tables 5.2 and 5.3, where a considerable dissolution structure was found after the experiment, cf. Section 5.6.

5.4. Permeability determinations

During experiment OCD1 the permeability of the composite sample was determined several times at different conditions. Table 5.5 gives a summary of the permeability determinations and the conditions of the measurements. The nitrogen viscosity is a literature value, the Isopar-L viscosity is interpolated from measurements at GEUS, the viscosity of the crude oil was determined during Step 9 of the experimental procedure (Table 5.1) when the Isopar-L oil within the sample was exchanged with crude oil. The viscosity of water at reservoir conditions was interpolated from measurements on similar fluids.

The initial and final gas permeability values show an increase of 23 % during the flooding experiment (Table 5.4) which is consistent with the evidence for slight dissolution of the grain material. The increase was evenly distributed between the individual sub-samples, cf. Tables 5.2-5.3.

The difference between permeability to gas and permeability to oil is within the usual range

Table 5.5. OCD1, permeability determinations.

	Sample state	Fluid	Perm (mD)	Flow rate (ml/h)	Temp (degree C)	Pconf (barg)	Pfluid (barg)	Viscosity (cP)
Individual samples:								
Initial perm	Sg = 100%	Nitrogen	0.622	n.a.	23	28	0.5	0.0176
Compound sample:								
Initial perm	Swi	Isopar-L	0.228	2.0	23	30	5	1.431
Initial perm	Swi	Isopar-L	0.217	2.0	85	30	5	0.602
After ageing	Swi	Dan crude	0.139	0.41	85	428	281	3.75
End waterflood	Sor	Water	0.0319	0.62	85	428	281	0.460
Start CO2-enr.flood	Sorco2	Water	0.0328	0.62	85	428	281	0.460
End CO2-enr.flood	Sorco2	Water	0.0318	0.62	85	428	281	0.460
Individual samples:								
Final perm	Sg = 100%	Nitrogen	0.765	n.a.	23	28	0.5	0.0176

for low-permeability chalk. Please note that the oil permeabilities of Table 5.5 are measured at $S_{wi}=22\%PV$. The permeability to Isopar-L laboratory oil was measured at 23 °C and again at 85 °C, with the two measurements being in good agreement. The permeability to Dan crude oil is significantly below the permeability to Isopar-L oil. The difference is considered mainly to reflect the pore volume reduction caused by the increased net overburden stress, but part of the difference may be caused by fluid redistribution within the pore system because of wettability changes during the ageing process. The permeability to water is again significantly below the permeability to Dan crude oil, reflecting the relative permeability conditions of the experiment.

5.5. Production of oil during the floodings

The production of fluids from the core was registered by the rig separator during the waterflooding and CO₂-enriched flooding operations. Table 5.6 gives a summary of the production of fluids during experiment OCD1. Table 5.7 presents the timing of important events during the floodings. The latter table also gives the elapsed time since the start of the floodings, and the fluid volume throughputs.

In spite of the very tight nature of sample OCD1, the waterflooding produced oil from the

Table 5.6. Oil production during experiment OCD1.

Sample OCD1	Oil prod. since previous step (ml)				Oil prod. since previous step (%PV)		Cumulate oil prod. during exp. (%PV)	Oil prod. during flood-ing (%PV)	Sw (%PV)	So (%PV)	Sg (%PV)
	Pore volume ¹⁾ (ml)	Water contents (ml)	Oil contents (ml)	Oil contents (ml)	Oil prod. during exp. (%PV)						
Initial state	-	91.64	20.41	71.24	-	-	-	22.3	77.7	0.0	
Waterflood:											
At breakthrough	40.60	91.64	61.01	30.64	44.30	44.30	44.30	66.6	33.4	-	
At end of waterflood	4.90	91.64	65.91	25.74	5.35	49.65	49.65	71.9	28.1	-	
CO ₂ -enriched flood without swelling correction											
End CO ₂ -enriched flood	3.00	91.64	68.91	22.74	3.27	3.27	52.92	75.2	24.8	-	
CO ₂ -enriched flood with swelling correction											
End CO ₂ -enriched flood	4.34	91.64	70.25	21.40	4.74	4.74	54.38	76.7	23.3	-	
Final Dean Stark											
Mean of individual samples	-	92.18	43.71	23.74	-	-	-	47.4	25.8	26.8	

Note 1: The column "Pore volume" gives the pore volume used for calculating oil production (%PV) and fluid saturation (%PV).

Table 5.7. OCD1 experiment. Timing of waterflood and CO₂-enriched flooding.

Sample pore volume is 91.64 ml.

Event	Time	Flooding time (hours)	Flooding time (days)	Through-put since start (ml)	Through-put since start (PV)
Waterflood					
Flowrate (ml/h) =	0.62				
Start of waterflood	05-jan-2007 08:38	0.00	0.00	0.0	0.00
Breakthrough	08-jan-2007 13:46	77.13	3.21	47.6	0.52
End of waterflood	07-feb-2007 10:13	793.58	33.07	490.1	5.35
CO ₂ -enriched flood					
Flowrate (ml/h) =	0.62				
Start of CO ₂ -enriched flood	16-feb-2007 14:14	0.00	0.00	0.0	0.00
End of CO ₂ -enriched flood	21-apr-2007 15:08	1536.90	64.04	949.2	10.36

sample quite efficiently. Water breakthrough occurred at a water saturation of 66.6 %PV. After breakthrough a further 4.9 %PV of oil was produced.

The CO₂-enriched flooding only produced relatively small amounts of oil. Using the separator data directly gives an additional oil production of 3.3 %PV. If a correction for oil swelling within the separator is made, the amount of additional oil during the CO₂-enriched flooding becomes 4.7 %PV. The latter value is recommended, see Section 5.7.

The fluid saturations given in Table 5.6 under the headings "Waterflooding" and "CO₂-enriched flood" are results of cumulative mass balance calculations using separator fluid volume data. The final Dean Stark analyses provide a check of the final separator fluid saturations by an independent method. The difference of 2.4 %PV between the separator oil saturation and the Dean Stark oil saturation reflects the combined effects of analytical uncertainty, any oil shrinkage or swelling that occurred during sample depressurization, and any oil lost from the sample during sample depressurization. The deviation of 2.4 %PV is considered satisfactory.

5.6. Waterflooding

A log of the OCD1 waterflooding is presented in Fig. 5.1. In Fig. 5.2 the same waterflooding data are presented plotted against injected water volume in PV (sample pore volume). Additionally, in Fig. 5.2 the separator oil volume of Fig. 5.1 has been recalculated to sample water saturation S_w . The flooding rate was 0.62 ml/h. Water breakthrough occurred on

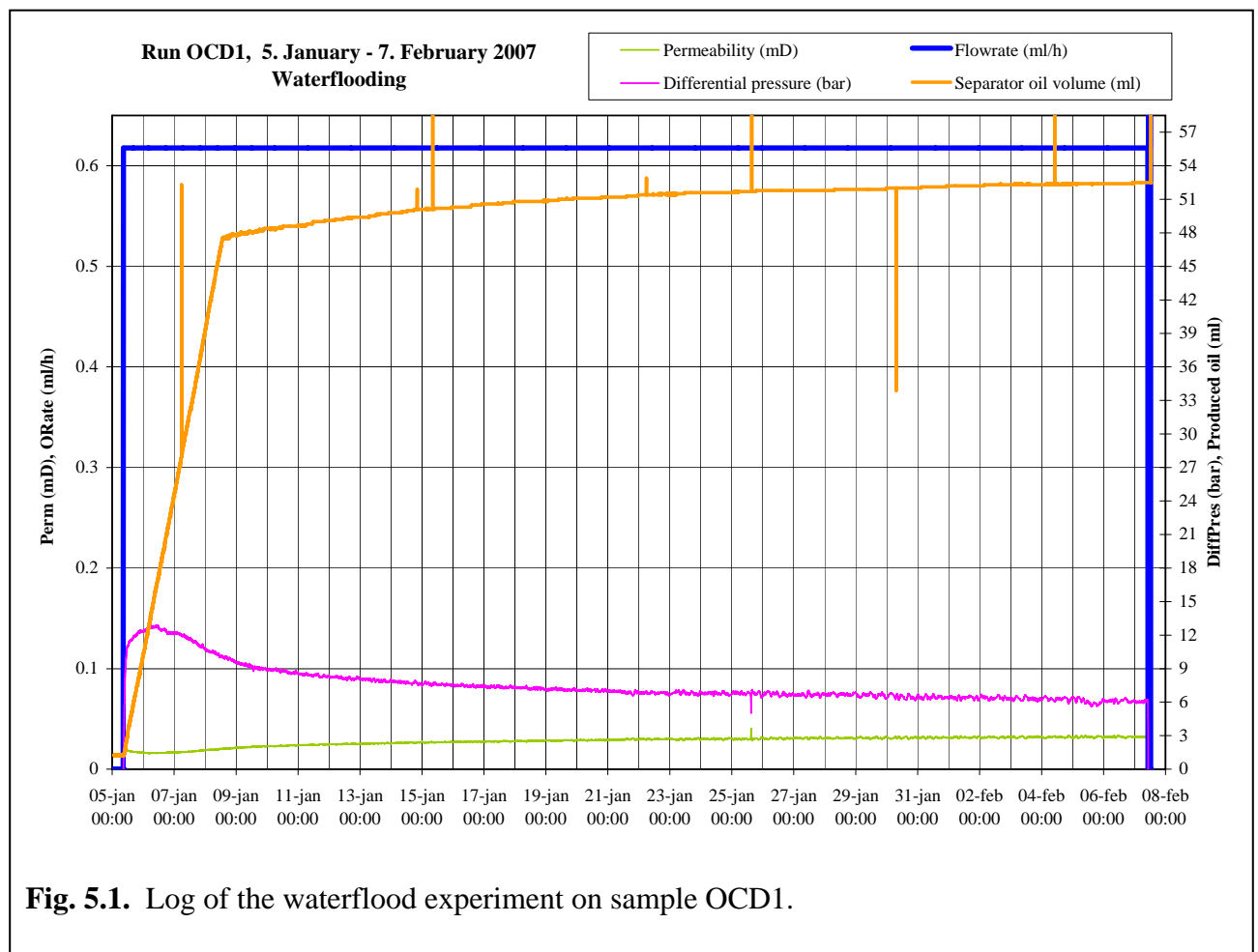


Fig. 5.1. Log of the waterflood experiment on sample OCD1.

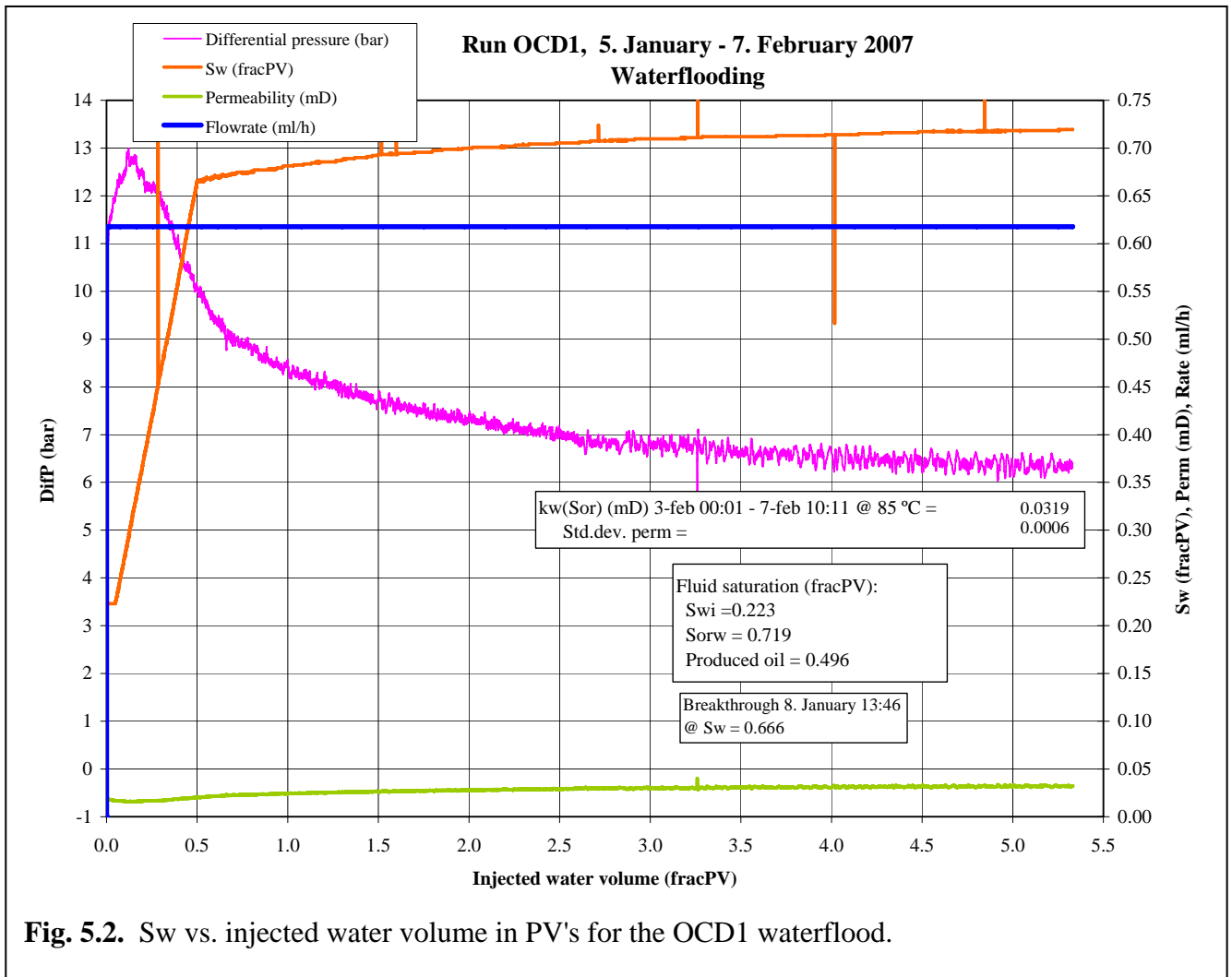
8. January 13:46, i.e. 77 hours after start of flow when the water throughput was 47.6 ml or 0.52 PV. After breakthrough the oil production dropped quickly, but a low oil production rate was sustained for a considerable time. Oil production had stopped completely when the waterflooding was terminated on 7. February after a total water throughput of 5.35 PV.

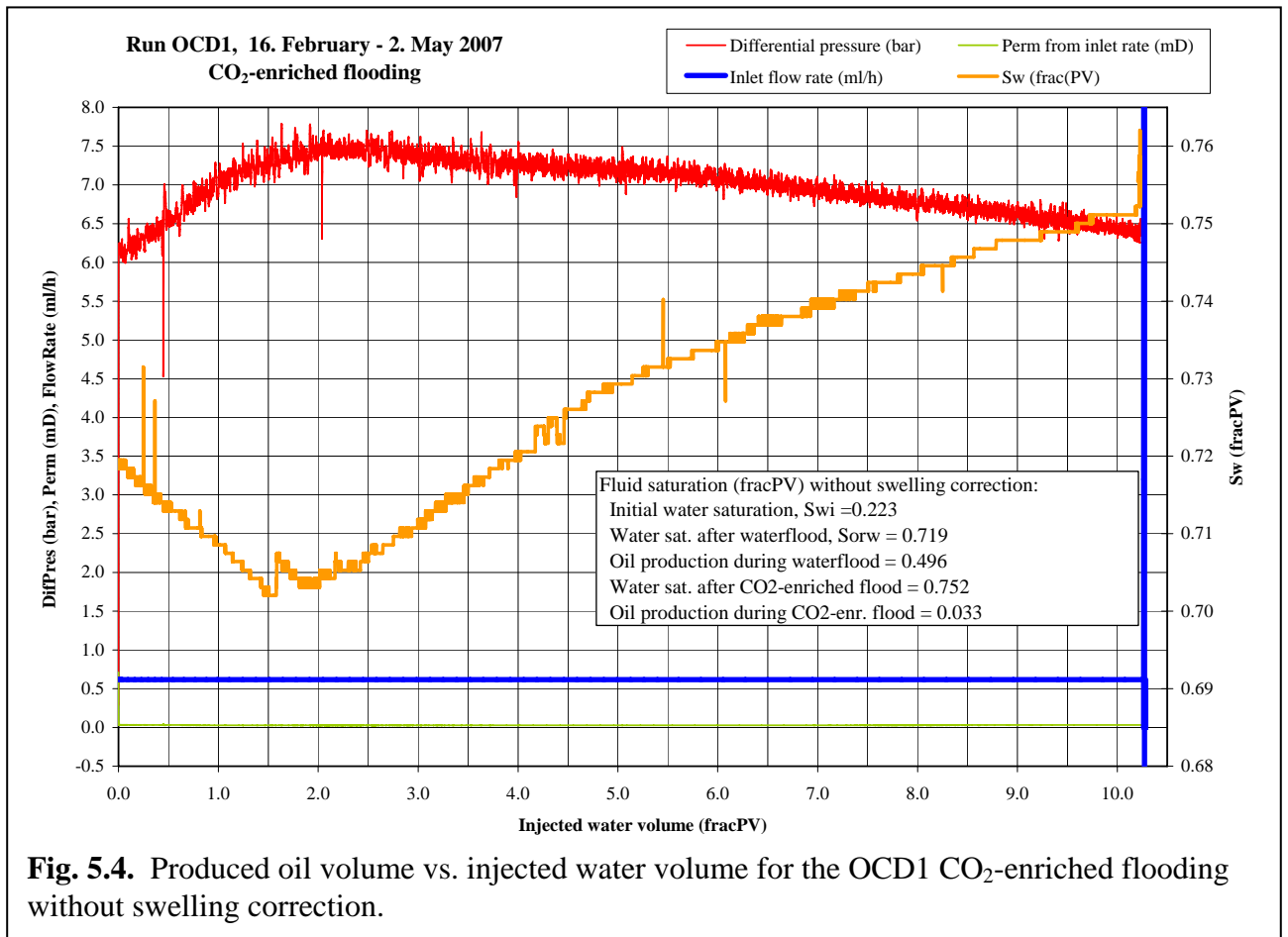
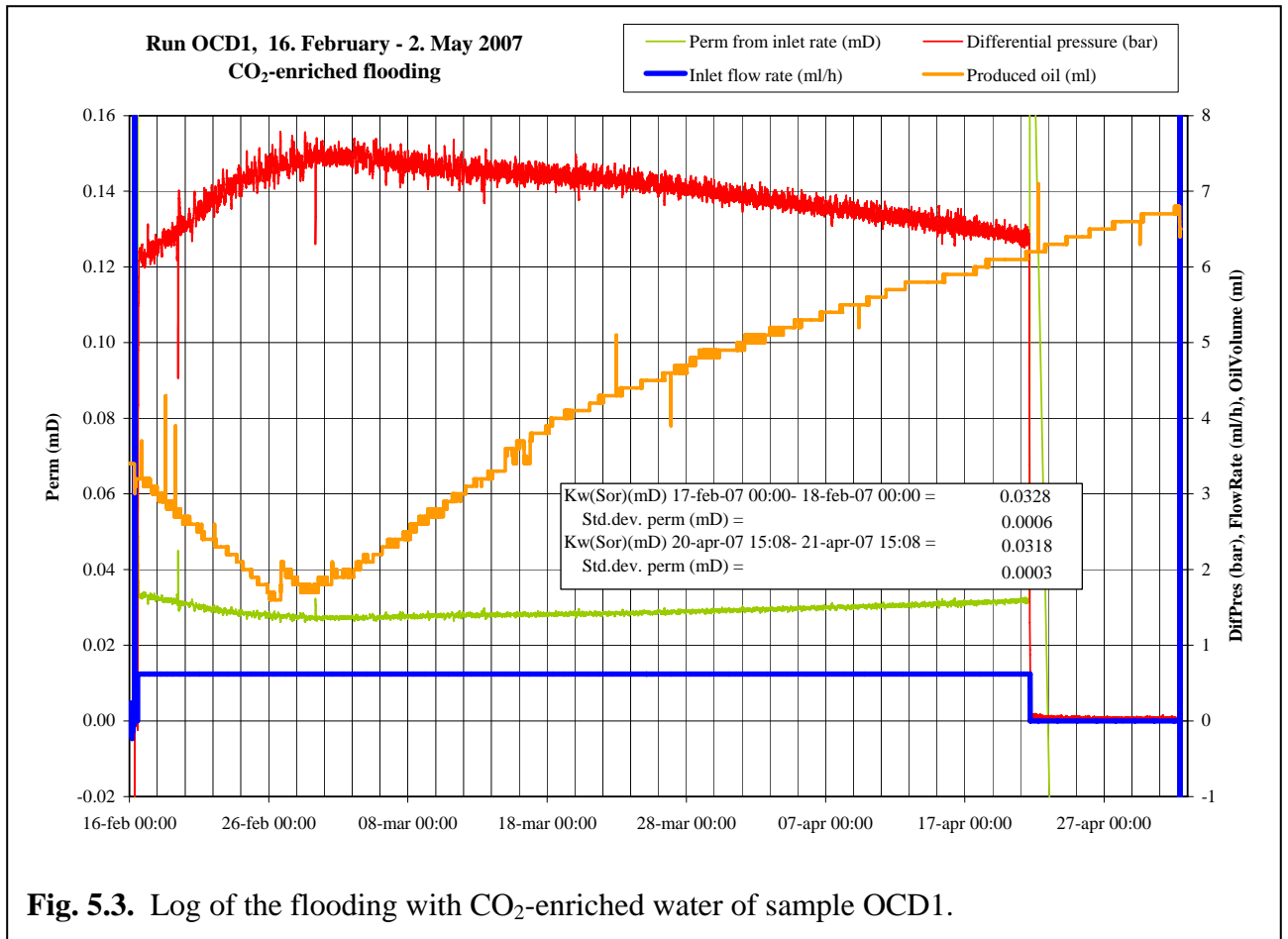
The differential pressure trace of Figs. 5.1 and 5.2 shows a typical waterflooding development. The peak differential pressure occurs well before water breakthrough because of the large difference in oil and water viscosity. At the end of the waterflooding the differential pressure had stabilized indicating the fluid movements within the sample had stopped.

5.7. CO₂-enriched flooding

Before the CO₂-enriched flooding (Step 13 of Table 5.1), CO₂ was added to the brine to saturate it 100 % with CO₂. From the data of Chang et al. (1998) the amount of CO₂ necessary to just saturate the brine was calculated to 26.6 Sm³ CO₂/Sm³ brine at the conditions of the experiment. This amount of CO₂ was added to the brine before starting the CO₂-enriched flooding.

Problems with disequilibrium between the oil and the CO₂-enriched water in the separator of the reservoir condition rig may arise in experiments with CO₂-enriched water.





The disequilibrium causes the oil within the separator to either swell or shrink when CO₂ diffuses between the two phases. Such volume changes are troublesome as they cannot be distinguished from oil being produced from the sample. In an attempt to avoid these problems an amount of CO₂ was added to the separator before starting the CO₂-enriched flooding. The amount of CO₂ was calculated to create the same CO₂-saturation within the water of the separator as in the brine used for flooding, which would eliminate disequilibrium.

A log of the CO₂-enriched flooding is presented in Fig. 5.3. In Fig. 5.4 the same flooding data are plotted against injected water volume in PV. Additionally, in Fig. 5.4 the separator oil volume of Fig. 5.3 has been recalculated to sample water saturation S_w. The flooding took place rate of 0.62 ml/h, which was the same rate as the waterflooding (Table 4.1).

Compared to the waterflooding, the amount of oil produced during the CO₂-enriched flooding was small. Small errors in the measurement of the oil production therefore become important.

It is evident that the oil production curve of Fig. 5.3 has a peculiar shape: Initially the curve has a negative slope, which indicates that the volume of oil in the separator was reduced. Because the construction of the rig prevents oil from flowing away from the separator, the negative slope of the production curve indicates that the oil in the separator shrank in volume during the first part of the CO₂-enriched flooding. After the section with negative slope, the slope of the oil production curve changes to positive and the curve gets the appearance of an ordinary oil production curve until the end of the flooding. However, oil appeared to be produced at a low rate right until the end of the flooding, which occurred after a total throughput of 10.36 PV of CO₂-enriched brine. To check the separator response, the rig was

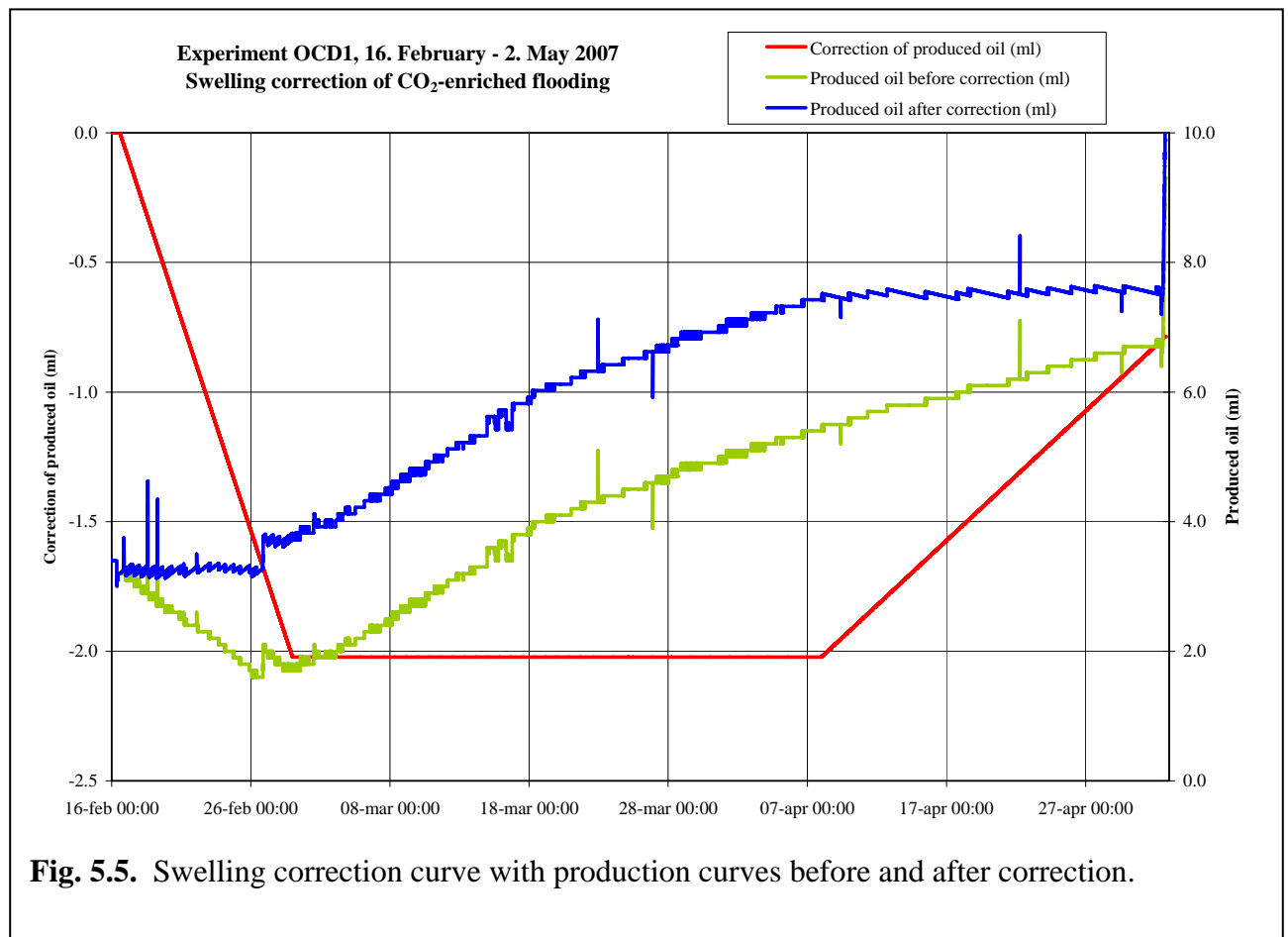


Fig. 5.5. Swelling correction curve with production curves before and after correction.

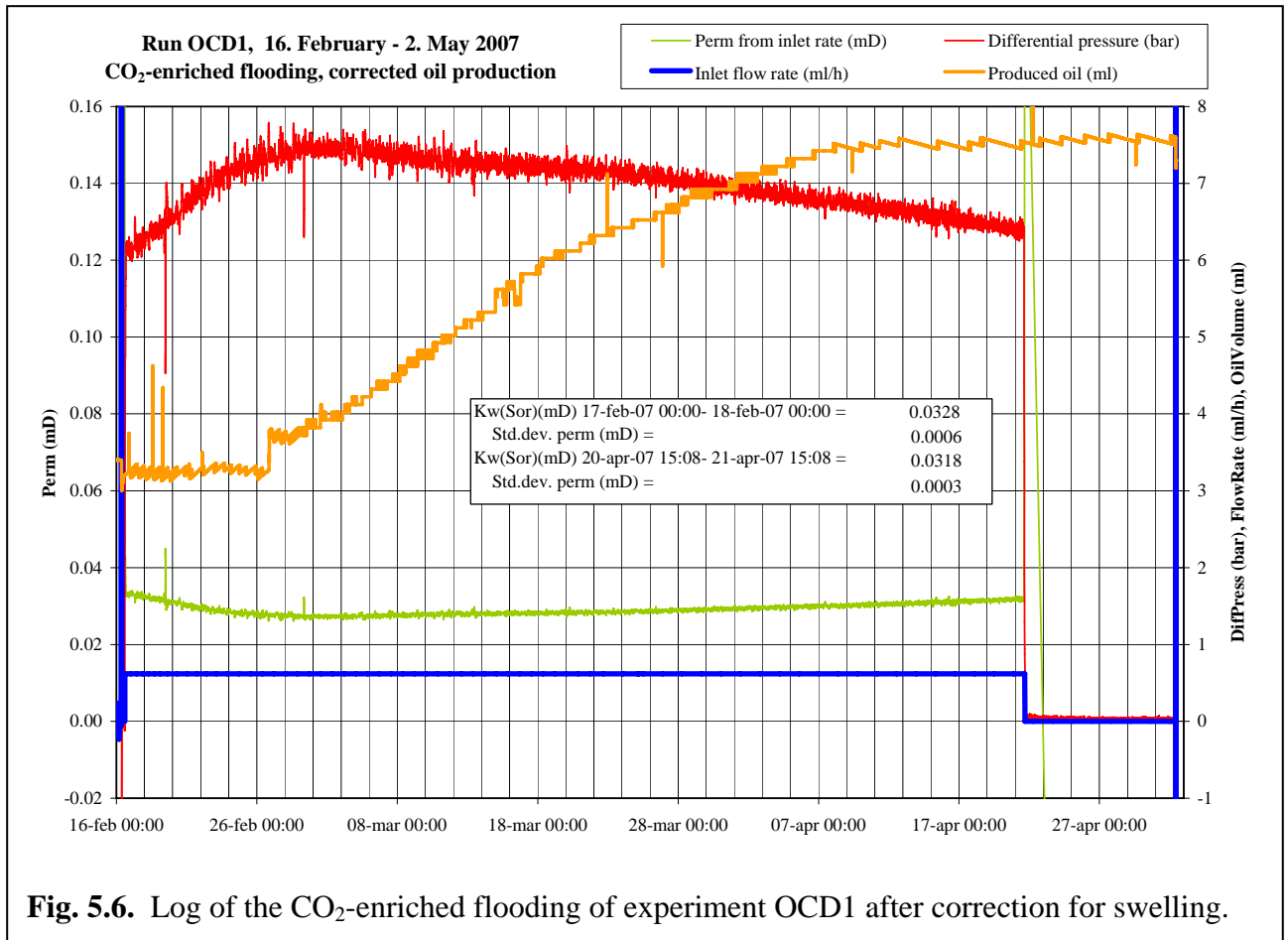
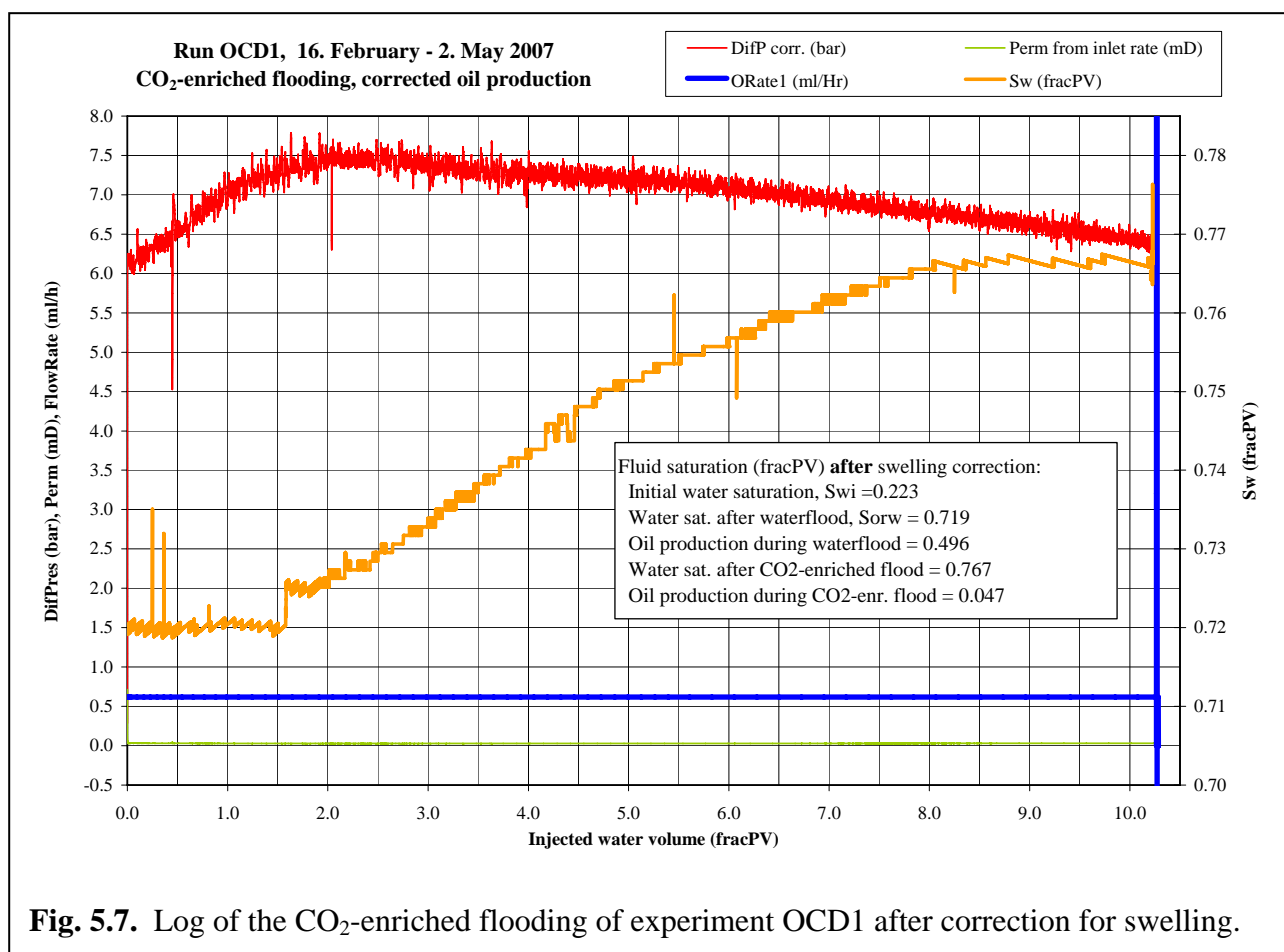


Fig. 5.6. Log of the CO₂-enriched flooding of experiment OCD1 after correction for swelling.

left without flow for 10.8 days after terminating the CO₂-enriched flooding. During this time the condition of the rig was the same as during the CO₂-enriched flooding, except that the fluid delivery pump was stopped. During this time the separator continued to register an increase in oil volume, at a rate that was similar to the rate during the final part of the CO₂-enriched flooding (Fig. 5.3). As the construction of the rig prevents that oil can flow to the separator when the delivery pump is stopped, the oil production after flow-stop is considered to represent swelling of the oil within the separator. The situation appears similar to the situation at the beginning of the CO₂-enriched flooding, only that swelling took place instead of shrinkage.

In a flooding with CO₂-enriched water it is expected that no oil is produced before somewhat less than 1 PV of water has been injected. It is therefore reasonable to assume that the section of the oil production curve with negative slope represents the time before breakthrough of the CO₂-enriched water and the first produced oil. The section with negative slope then should correctly be horizontal, i.e. indicating no oil production. Similarly, the section of the oil production curve lying after flow-stop should correctly be horizontal, i.e. also indicating no oil production. Using these arguments a swelling correction curve has been constructed that turns the two curve sections horizontal, cf. Fig. 5.5. As oil shrinkage clearly changed to oil swelling during the experiment a section with neither shrinkage nor swelling has been inserted in the correction curve. This latter part of the curve indicates equilibrium in the separator. The correction curve of Fig. 5.5 therefore consists of three linear segments indicating abrupt change from significant shrinkage to equilibrium, and again an abrupt change from equilibrium to significant swelling. The true correction curve probably is a curve



starting and ending with slopes as the curve in Fig. 5.5, but with gradually changing slope in between. However, as no evidence is available for the true shape of this curve the segmented curve of Fig. 5.5 has been chosen.

The evidence for shrinkage and swelling is interpreted as follows. At the start of the CO₂-enriched flooding the pore space of the sample contained 65.9 ml of CO₂-free water. During the first week of the CO₂-enriched flooding this water flowed to the separator and caused disequilibrium with the oil of the separator that shrank in volume as CO₂ diffused from oil to water. After break-through of the CO₂-enriched water, the CO₂ contents in the water of the separator gradually increased and after some time the direction of CO₂ diffusion changed and the oil of the separator started to swell.

Fig. 5.5 also shows the effect of the swelling correction on the oil production curve of the CO₂-enriched flooding. It is seen that the curve segment with negative slope is turned horizontal, and that the segment with positive slope after flow-stop is also turned horizontal. The part lying between these two segments has the shape of an ordinary oil production curve.

The log of the CO₂-enriched flooding (Fig. 5.3) is presented in Fig. 5.6 as it looks after application of the swelling correction. Similarly, the S_w vs. injected water curve of Fig. 5.4 is presented after application of the swelling correction as Fig. 5.7. The total oil production both with and without swelling correction is given in Table 5.6. Without correction for swelling the total oil production during the CO₂-enriched flooding was 3.27 %PV. After correction for swelling the total oil production was 4.74 %PV. No matter whether the correction procedure

is used or not, the amount of additional oil produced by the CO₂-eriched flooding is small compared to the amount of oil produced by the waterflooding.

5.8. Compaction and dissolution structures

During experiment OCD1 the position of the floating end piece of the core-holder was determined a number of times. The determinations were made manually with a digital caliper at convenient times, i.e. at times when the thermal disequilibrium created by the determination did not disturb other parts of the experiment. Fig. 5.8 presents a log of the caliper results.

During the period from just before pressurization to just before starting the waterflood the sample showed a length reduction of 0.6 mm. This length reduction is considered to represent the combined effect of core holder settling and elastic compression of the sample.

During the waterflooding the sample length was only reduced by 0.08 mm. This is actually below the accuracy of the determination which is 0.1 mm. During the CO₂-enriched flooding a length reduction of 0.58 mm was recorded that is clearly caused by the flooding. The combined length reduction during waterflooding and CO₂-enriched flooding is 0.66 mm, which compares well with the length reduction of 0.74 mm calculated from the initial and final sample characterization, cf. Table 5.4.

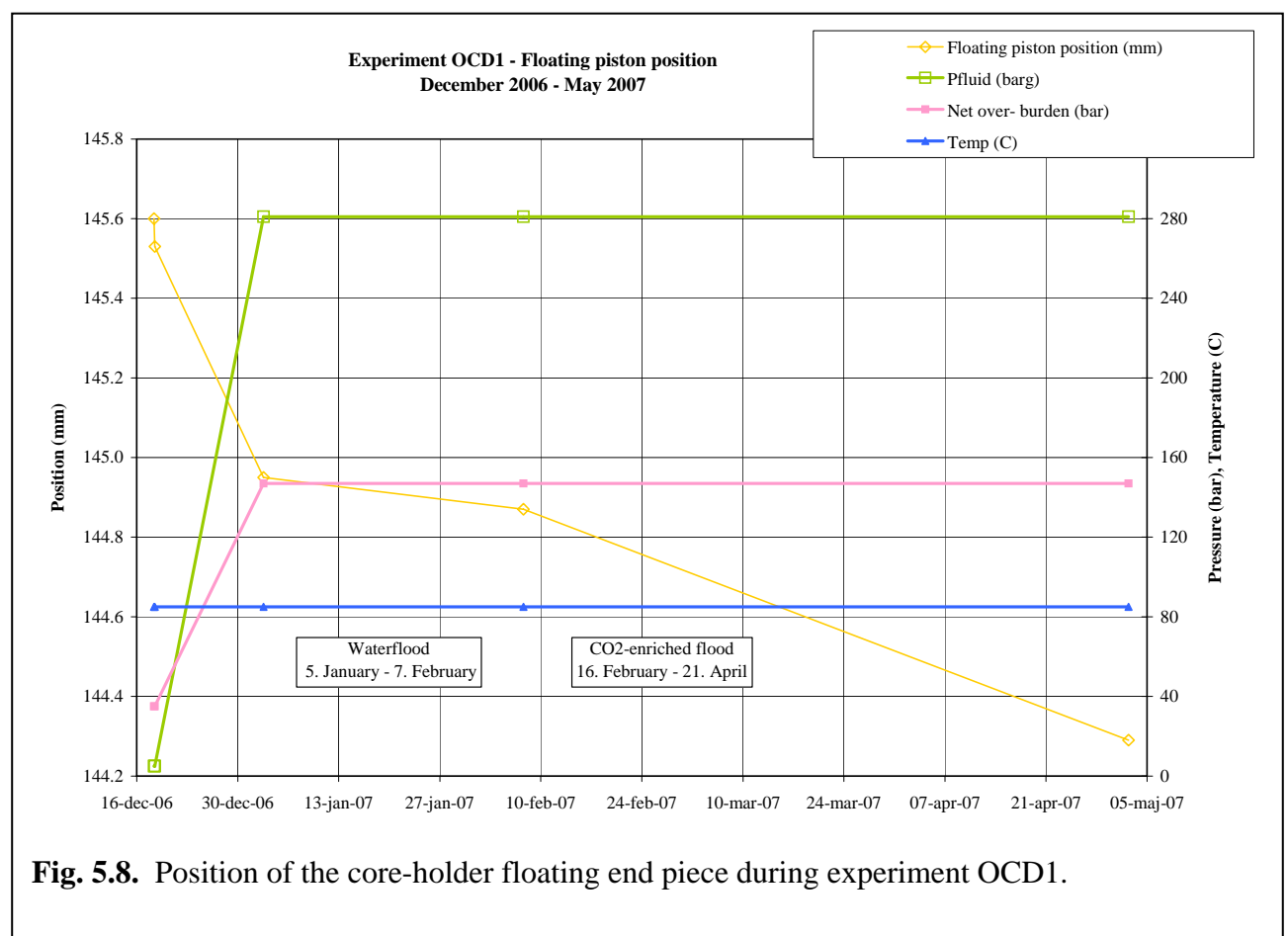


Fig. 5.8. Position of the core-holder floating end piece during experiment OCD1.

After experiment OCD1, the inlet end face of composite sample OCD1 contained a dissolution structure that was not present before the experiment, Fig. 5.8. The structure is undoubtedly caused to dissolution by the brine during the CO₂-enriched flooding. Dissolution structures were only present on the inlet face of the composite sample. The outlet face of the composite sample did not show signs of dissolution, and the same applies to all the end faces separating the four sub-samples of the composite sample. The evidence shows that the reaction rate of the CO₂-enriched brine was so large that a significant part of the reactions occurred when the brine passed through the inlet end face.



Fig. 5.9. Inlet end of composite sample OCD1 after flooding with CO₂-enriched water. Sample diameter is 37.65 mm. The mesh pattern adjacent to the margin of the sample is an impression of the inlet filter of the core holder.

6. References

Chang, Yih-Bor, Coats, B.K. & Nolen, J.S. (1998): "A Compositional Model for CO₂ Floods Including CO₂ Solubility in Water", *SPE Reserv. Eval. Eng.*, **1,2**, p. 155-160, 1998.

Jorgensen, L.N. (1991); "Dan Field -Denmark, central Graben, Danish North Sea", in *Foster, N.H. & Beaumont, E.A. (eds.): Atlas of Oil and Gas Fields, AAPG, Tulsa OK, U.S.A, p .199-218.*